Special features of high energy hadrons in air showers

1973 J. Phys. A: Math. Nucl. Gen. 6 1050

(http://iopscience.iop.org/0301-0015/6/7/026)

J. Phys. A: Math., Nucl. Gen., Vol. 6, July 1973. Printed in Great Britain.

Special features of high energy hadrons in air showers

R H Vatcha and B V Sreekantan

Tata Institute of Fundamental Research, Bombay-5, India

Received 7 December 1972

Abstract. The properties of hadrons of energy $2{\cdot}5 \times 10^{10}$–10^{13} eV in air showers of size 5×10^4–3×10^6 particles at 800 g cm^{-2} have been studied using a 2 m^2 multiplate cloud chamber as the hadron detector operated at the centre of the TIFR air shower array at Ootacamund. The results show a tendency for the lateral distribution of high energy hadrons to flatten with increasing shower size. The energy spectrum in the range 50–800 GeV steepens continuously with size and the number of hadrons does not increase linearly with size, but at a much slower rate especially for high energy hadrons. The fractional energy spectrum of hadrons of energies greater than 200 GeV is different for showers of size less than and greater than 3×10^5 particles. The charge to neutral ratio of hadrons of energy greater than 25 GeV in showers of size less than $3{\cdot}2 \times 10^5$ is found to have a rather low value ($6{\cdot}2 \pm 1{\cdot}3$) and there is evidence for a further decrease in this value for larger size showers. While a comparison of the present results with those of others is presented in this paper, the interpretation of the results in terms of primary composition and the characteristics of high energy interactions is reserved for two subsequent papers.

1. Introduction

With the advent of intersecting storage rings at CERN, it has now become feasible to extend observations on the characteristics of p–p collisions up to energies of the order of 2×10^{12} eV. However, there is considerable interest and need to know the behaviour of strong interactions at still higher energies especially from the point of view of the interpretation of cosmic ray phenomena at the highest energies and also for verifying the asymptotic validity of scale invariance theories (Feynman 1969). With the help of extensive air showers (EAS) it is possible to extend the study of the characteristics of strong interactions up to very high energies. The low flux of primary cosmic rays is compensated in EAS studies by large detection areas that become effective as a result of the spread of the secondary particles. However, due to the complexity of the air shower phenomenon, the interpretation of results is not straightforward. A major problem arises in distinguishing the effects of primary composition from those of collision characteristics. Several investigators have carried out detailed Monte Carlo simulations of air showers to identify features which are exclusively sensitive to either the mass of the primary nucleus initiating the shower or to the characteristics of ultra-high energy collisions. It has become apparent that it is only through a number of iterative stages of study of the correlations between the different components and the internal consistency in their behaviour that the complex effects of these two aspects can be segregated and knowledge concerning both gained. Among the various secondary components the two which are particularly sensitive to changes in primary composition and collision characteristics are the high energy hadrons which constitute the back-bone and skeleton of air showers and the ultra-high energy muons which arise predominantly in the first few collisions at the top of the atmosphere.

The situation concerning the experimental data on high energy hadrons in air showers is far from satisfactory. The high energy hadrons are concentrated in regions close to the core and their number is quite low. The hadron detector assemblies are necessarily complicated since they have not only to detect hadrons, but also measure their energy. Among the non-visual type of hadron detectors, transition chambers, ionization calorimeters and total absorption spectrometers have been used. These suffer the disadvantage that they do not enable the separation of charged hadrons from neutral ones, and events caused by the incidence of multiple particles from those caused by single hadrons. Multiplate cloud chambers offer a distinct advantage in this respect. However, there are very few experiments that have been carried out using cloud chambers. Besides there exists considerable disagreement between the results of different experiments using different types of detectors for studying the high energy hadrons in EAS (see, for example, Murthy 1967).

We have studied the properties of hadrons of energy greater than $2{\cdot}5 \times 10^{10}$ eV in air showers of size 5×10^4–3×10^6 particles using a 2 m^2 multiplate cloud chamber, at the centre of the Ooty air shower array. In this paper we present briefly the experimental details and the methods of analysis of data, and give a fairly comprehensive account of the experimental results that we have obtained and then make a comparison of the results with those of other experiments and point out certain special features in the variation with shower size of some properties of the high energy hadronic component. In accompanying papers we consider the interpretation of these results in the light of the Monte Carlo simulations that exist on the hadronic component of proton and heavy primary induced EAS and discuss the trends in the characteristics of strong interactions at ultra-high energies which are needed to explain the observed results.

2. Experimental details

The TIFR air shower array at Ooty (800 g cm^{-2}) which is designed for recording showers in the size range 5×10^4–5×10^6 particles is shown in figure 1. The full details are available elsewhere (Vatcha 1972). For individual showers in this size range the array provides information on the position of the axis, the shower size, the direction of arrival and also the value of the steepness parameter α_e, in the lateral distribution function of electrons given by

$$\Delta(r) = \frac{N_e}{2\pi r_0^2} \frac{\exp(-r/r_0)}{(r/r_0)^{\alpha_e}\Gamma(2-\alpha_e)}.$$

The values of core position, shower size and α_e are obtained by a χ^2 minimization procedure using a CDC-3600 computer. The direction of arrival is determined by the usual fast-timing technique.

The hadron detector located at the centre of the array is a large multiplate cloud chamber of dimensions 2 m × 1·5 m × 1 m with 21 iron plates inside, each of 2 cm thickness corresponding to a radiation length, and the whole plate assembly corresponds to about 2·2 interaction mean free paths. The chamber is shielded on the top by an absorber equivalent to about 5·5 radiation lengths of iron and lead.

The method of estimating the energy of hadrons interacting in the chamber has been described in detail in an earlier paper (Vatcha *et al* 1972). For cascade energies less than 200 GeV, it is feasible to count individual tracks and the energy is determined by evaluating the track length integral. For higher energy cascades a new method of

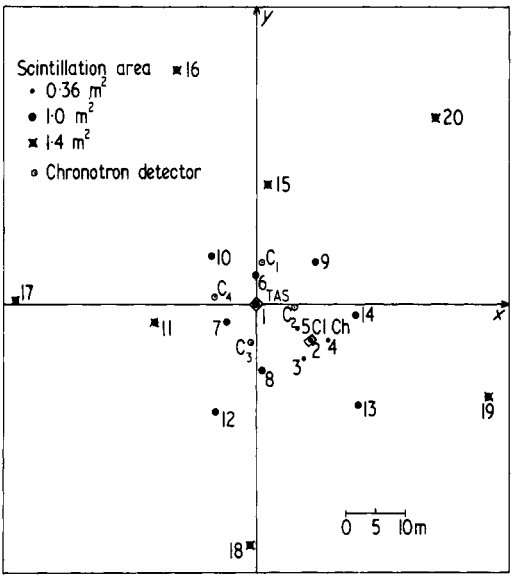

Figure 1. The extensive air shower array at Ootacamund.

evaluating the track length integral by measuring the 'saturated widths' of the cascades at different stages of development, and using Monte Carlo simulations for calibrations has been developed and used. The statistical error in the energy estimate of hadrons is better than 50% up to the highest energies. It has been shown elsewhere (Vatcha 1972) that due to some uncertainty in the measurements of saturated widths there may be a systematic underestimate of hadron energies. The maximum probable underestimate is about 50%.

The cloud chamber was operated in association with the air shower array from August 1968 to February 1969 and from November 1969 to September 1970. A total of 20 000 showers was recorded in an effective operation time of 6800 hours using different electron density criteria for air shower selection. The details regarding the operational features, the method of analysis of cloud chamber photographs, the classification of data, the selection criteria, evaluation of the 100% efficiency areas, the efficiency of the hadron detector for different angles of incidence and the evaluation of errors in the different parameters etc are available elsewhere (Vatcha 1972). The procedure used for evaluating the flux of hadrons automatically takes into account the effects of angular distribution of showers and is insensitive to the exact value of interaction mean free path of hadrons in iron. In addition to the cloud chamber, the total absorption spectrometer, TAS (located at a distance of about 11 m from the cloud chamber), described elsewhere (Ramana Murthy *et al* 1963) was also operated during the entire period as a second hadron detector and this enabled a comparison of data on hadrons from visual and non-visual detectors in the same experiment.

2.1. The lateral distribution of hadrons

For detailed analysis the size interval $5{\cdot}6 \times 10^4$–$5{\cdot}6 \times 10^6$ particles is divided logarithmically into 8 sub-intervals. The distance interval between the shower axis and the cloud chamber which extends mostly up to about 32 m is divided such that the Rth interval

extends from $2^{(R-1)/2}$ m to $2^{R/2}$ m. The hadron energy intervals are classified such that the nth interval extends from $25 \times 2^{n-1}$ GeV to 25×2^n GeV. The steepness parameter is classified into 5 equal sub-intervals extending from 0 to 2·0. The density of hadrons per shower in any particular sub-group is given by

$$\Delta(N_e, r, > E_H) = \frac{H(N_e, r, > E_H)}{N(N_e, r)} F$$

where H is the observed number of hadrons in the bin of average size N_e, average distance r and hadron energy greater than E_H; N is the observed number of showers in the same bin and F is the geometrical factor of the cloud chamber.

The densities of hadrons obtained in this way were compared for different triggers to check the bias due to triggering inefficiencies at different core distances. No appreciable difference for the different triggers was found. This was further verified by calculating the average values of 'α_e' for different triggers and for different size and distance groups. Therefore data from all density triggers were combined to obtain the lateral distribution and some typical cases are plotted in figure 2 for hadrons of energies greater than 50 GeV

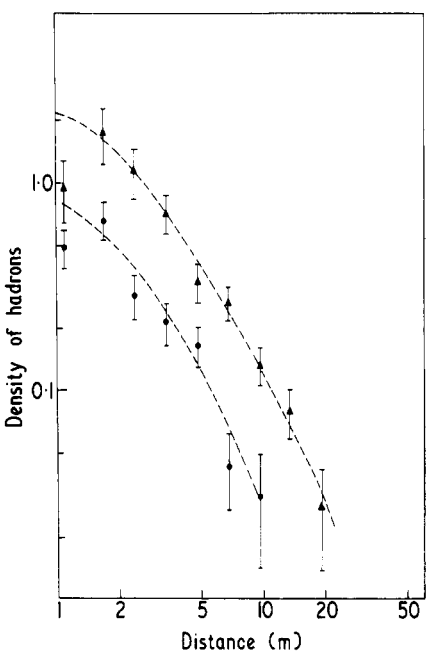

Figure 2. The lateral distribution of hadrons (> 50 GeV) associated with EAS in two typical size groups: $1{\cdot}8 \times 10^5$–$3{\cdot}2 \times 10^5$ (●) and 10^6–$1{\cdot}8 \times 10^6$ (▲). The broken curves are the best fits to the experimental points.

for two size regions. The distributions are similar at other sizes and energies. The experimental points are fitted using the formula

$$\Delta_n(r) = \frac{N_n}{2\pi r_n^2} \frac{\exp(-r/r_n)}{(r/r_n)^{\alpha_n}\Gamma(2-\alpha_n)}$$

where Δ_n is the hadron density at a distance r, N_n is the total number of hadrons for the

given shower size and α_n, r_n are two free parameters with α_n subject to $0 < \alpha_n < 2$. The χ^2 minimization is done in two stages; in the first stage α_n is fixed. The value of N_n is not seriously affected by small deviations in values of r_n and α_n since the χ^2 surface is very flat over a large range of coupled values of r_n and α_n. Values of N_n obtained in this way are compared with values of N_n within 20 m of the shower core obtained by adding contributions from different distance groups directly. N_n (total) and N_n ($\leqslant 20$ m) agree reasonably well at lower sizes but increasingly disagree at higher sizes. This implies that a larger fraction of hadrons lie outside 20 m at higher sizes or in other words, the lateral distribution of hadrons flattens with increasing size. This feature is illustrated in figure 3 where the lateral distributions are plotted normalized to a constant

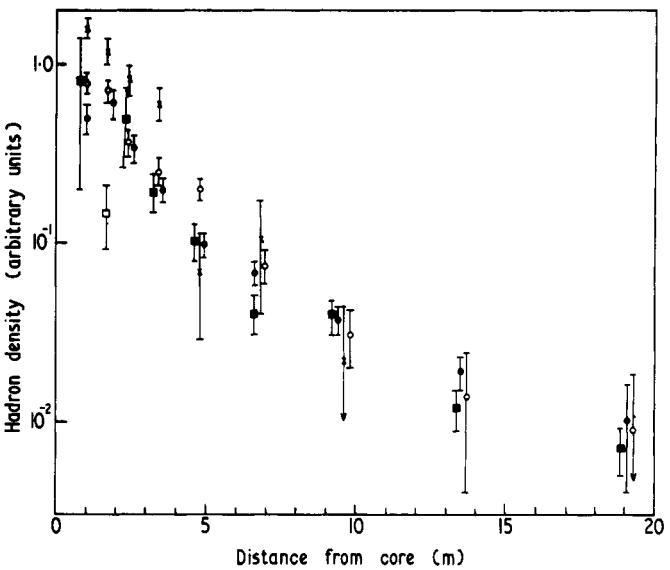

Figure 3. The normalized lateral distributions of hadrons (> 50 GeV) associated with EAS in different size groups: × about $5{\cdot}0 \times 10^4$–$1{\cdot}3 \times 10^5$; ○ $1{\cdot}8 \times 10^5$–$5{\cdot}6 \times 10^5$; ● $5{\cdot}6 \times 10^5$–$1{\cdot}8 \times 10^6$; ■ $1{\cdot}8 \times 10^6$–$5{\cdot}6 \times 10^6$. The areas under the curves for different size groups are normalized and at distances near the core the densities of the larger size groups are less than those of the smaller size groups.

N_n (total) for all size groups. At smaller distances, the points corresponding to the hadron densities in larger size groups lie in general below those due to smaller size groups. As the areas under the curves are normalized this again indicates a flattening of the lateral distribution with increasing size. Due to poor statistics it is difficult to make a quantitative evaluation of this trend.

2.2. Laterial distribution of cascades of energy greater than 1 TeV

During the 6800 hours of observation a total of 28 events due to hadrons of energies greater than 1 TeV were recorded in the chamber. Out of these 10 were associated with showers of size less than 3×10^5 and 18 with showers of size greater than 3×10^5. The lateral distribution of these events is given in table 1 and the energies of the individual hadrons are also listed. It is seen that hadrons with energies greater than a few TeV

Table 1. Lateral distribution of TeV cascades

Distance from core (m) r / Shower size	0–1·4		1·4–2·0	2·0–2·8	2·8–4·0	4·0–5·6
$< 3 \times 10^5$	9/517		1/362	0/413	0/496	0/493
	1·8 TeV	2·0 TeV	1·5 TeV			
	2·2 TeV	2·5 TeV				
	70·0 TeV	150 TeV				
	9·0 TeV	2·5 TeV				
		2·5 TeV				
$> 3 \times 10^5$	11/176		2/182	2/275	2/490	1/788
	1·0 TeV	2·0 TeV	4·7 TeV	1·1 TeV	9·4 TeV	
	1·0 TeV	1·1 TeV	1·1 TeV	1·4 TeV	1·7 TeV	2·4 TeV
	2·0 TeV	2·6 TeV				
	3·5 TeV	2·6 TeV				
	1·4 TeV					
	9·0 TeV	15·0 TeV				
	1·0 TeV					

have been recorded up to a distance of 5·6 m from the core. On the basis of artificial shower analysis (for details see Vatcha 1972) the fraction of showers expected at distances greater than 1·4 m due to errors in shower axis determination for the two size groups has been calculated and is given in table 2, and compared with the observed fractions.

Table 2. Effect of core location errors on lateral distribution of TeV cascades

Size	Expected number of showers at distances $> 1{\cdot}4$ m	Observed number of showers at distances $> 1{\cdot}4$ m
$< 3 \times 10^5$	$(7 \pm 3)\%$	1/10
$> 3 \times 10^5$	$(7 \pm 2)\%$	7/18

It is seen that for the size group less than 3×10^5 the observed distribution can be explained in terms of core location errors. For the larger size group, however, it looks unlikely that the observed distribution can be accounted for in terms of core location errors, especially since in this case the distribution would fall off rather sharply. Whether these high energy events occurring at large distances from the core constitute evidence for large p_T will be discussed in a later paper.

2.3. The variation of the number of hadrons with size

The variation of the number of hadrons per shower as a function of shower size has been determined for different threshold energies of hadrons and is shown in figure 4. The hatched† areas represent the degree of uncertainty due to a possible systematic

† Henceforth this convention will be adopted.

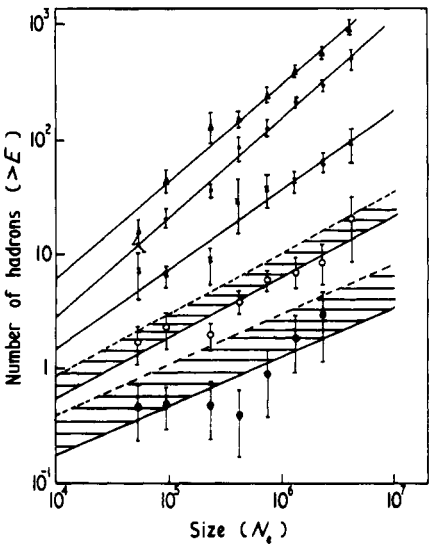

Figure 4. The variation of the number of hadrons of different energy thresholds 'E' with shower size. Values of E (GeV) are: 25; 50; 100; 200; 400. The straight lines are the least-square fits. The hatched regions pertaining to hadrons of energies greater than 200 GeV and greater than 400 GeV indicate the effects of a maximum probable underestimate in the energy of such hadrons.

underestimation in the hadron energy as described earlier. The full lines in the figure are the least-square fits to the equation

$$N_n(>E) = AN_e^{\alpha(E)}$$

in the size interval 5×10^4 to 3×10^6 particles. The results show an interesting trend. The *average* slope in this size region decreases with increasing hadron energy. It may be emphasized that any systematic error in the determination of the hadron energy can only change the value of the threshold energy but will not change the trend regarding the variation of $\alpha(E)$ with size, since the systematic error is not coupled to the size in the present cloud chamber experiment. In the case of experiments with non-visual hadron detectors, there could be a correlation between hadron energy estimate and shower size.

For hadrons of high energies there is even an indication of a break in the slope at a size $(3\text{–}4)\times10^5$. Below this size there is very little variation of N_n with N_e whereas the slope steepens above this size. The progressive flattening could be the result of such a break. It should be emphasized, however, that the statistical significance is not sufficient to claim a *definite* break on the basis of data for individual energy groups.

2.4. Integral energy spectra of hadrons (25–800 GeV)

The integral energy spectra of hadrons in the energy range 25–800 GeV in showers of size 7×10^4 to $3{\cdot}2\times10^6$ particles are given in figures 5(*a*, *b*). To provide clarity in the figures, the spectra for alternate size groups are plotted in parts (*a*) and (*b*).

In the energy range 50–800 GeV, the hadron spectra are represented by

$$N_n(>E) = BE^{-\gamma(N_e)}$$

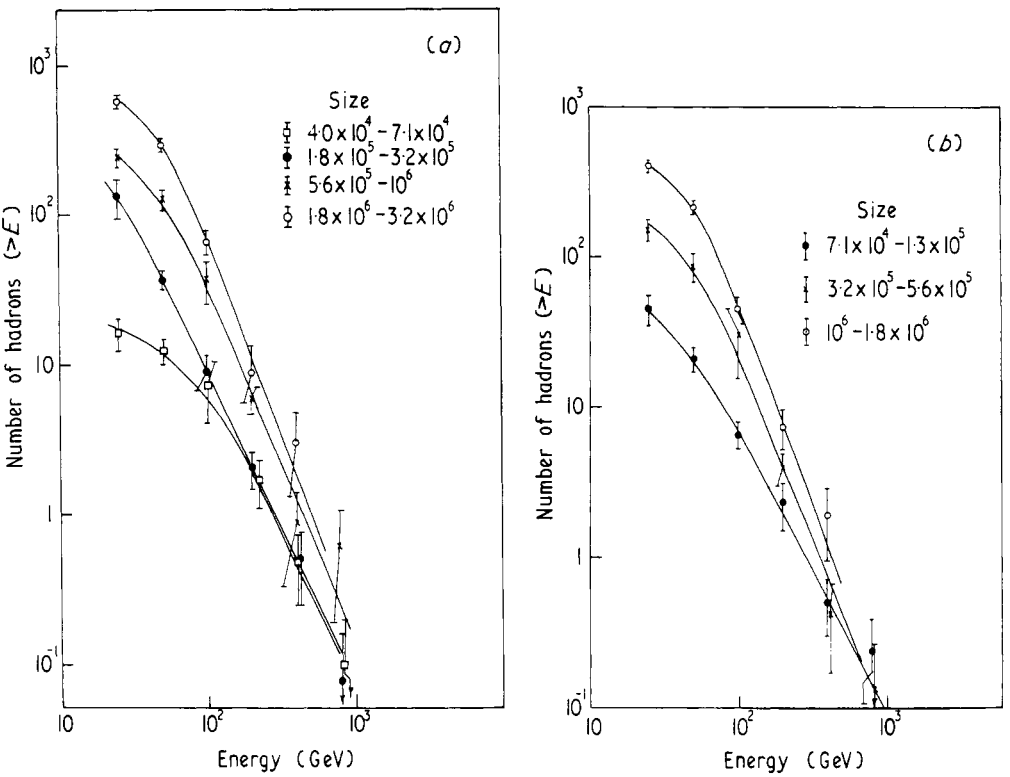

Figure 5. The integral energy spectrum of hadrons of energies from greater than 25 GeV to greater than 800 GeV associated with EAS of sizes ranging from 4×10^4 to $3{\cdot}2 \times 10^6$. For clarity alternate size groups are given in parts (*a*) and (*b*).

where the exponent γ is a function of shower size. The variation of γ with N_e is shown in figure 2 of paper III (curve A). It is seen that γ increases with N_e up to $3\text{–}4 \times 10^5$ particles and remains constant thereafter. Curve B in figure 2 of paper III is drawn after correcting for possible systematic underestimates of energy. It is seen that the tendency for γ to increase and flatten at a few times 10^5 is unaffected even after this correction.

There could be a slight bias in the experiment in determining the number of hadrons in the energy range 25–50 GeV in large air showers as some of these could be missed in the background of multiple high energy cascades. However the lateral distribution is flat enough for the total number not to be affected seriously. The variation of $\alpha(E)$ with E (§ 2.3) for showers in the size range 5×10^4–3×10^6 is shown in figure 6. It is seen that $\alpha(E)$, which has a value of about 0·8 up to 50 GeV, continuously decreases and has a value of about 0·4 at $E > 400$ GeV. The points with broken error bars are obtained after correcting for possible systematic errors in energy estimate. It is seen that this correction does not change the trend.

2.5. Energy spectra of very high energy hadrons

The very high energy events have been classified into only two size groups corresponding to average primary energies of about 3×10^5 GeV and approximately 2×10^6 GeV since the numbers are small. The averaged integral energy spectra for the two groups

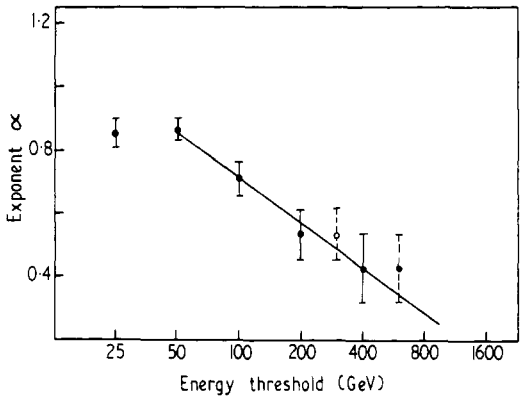

Figure 6. The variation with threshold energy of the exponent α which pertains to the size variation of the number of hadrons. $N_c = 5 \times 10^4$–5×10^6. The points with broken error bars are obtained after correcting for energy underestimate as explained before.

are shown in figure 7. There is a small bias introduced in the process of averaging since the lateral distribution of very high energy hadrons is steep and smaller size EAS are triggered preferentially close to the cloud chamber, so that the average weighted size decreases slightly as the hadron energy increases. When the energy spectrum is very steep it is essential to consider the effects of statistical errors in energy estimates of hadrons on the spectrum. If the true energy spectrum is given by $N_n\,(>E) = BE^{-\gamma}$,

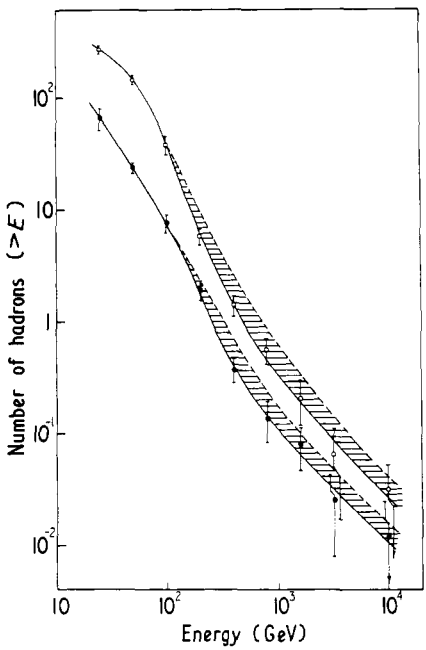

Figure 7. The integral energy spectrum of hadrons of energies from greater than 25 GeV to greater than 10 000 GeV associated with EAS of two size groups: ● $4{\cdot}0 \times 10^4$–$3{\cdot}2 \times 10^5$, average primary energy = 3×10^5 GeV; ○ $3{\cdot}2 \times 10^5$–$3{\cdot}2 \times 10^6$, average primary energy = 2×10^6 GeV. The hatched regions indicate the effects of energy underestimate as explained before.

then the observed spectrum would be as a result of statistical errors of the form

$$N_n(>E) = BE^{-\gamma}\{1-\beta+\tfrac{1}{2}\beta(2^{\gamma}+2^{-\gamma})\}$$

where β represents the fraction of hadrons transferred to the neighbouring energy channels (defined earlier) due to statistical errors in energy estimate. In deriving this relation, it is assumed that β is symmetrically distributed as is approximately indicated by the Monte Carlo simulations of hadronic cascades in the chamber (Vatcha 1972). In our case $\beta \simeq 0{\cdot}3$ to $0{\cdot}5$, and as γ approaches a value around 2, the actual number of hadrons $N_n(>E)$ may be smaller by about 35%. However, a detailed comparison of cascade profiles observed in the cloud chamber with those expected from Monte Carlo simulations has shown that the method adopted in obtaining hadron energies leads to a systematic underestimate by about 20% for hadrons of energies less than 200 GeV. Therefore we believe that this underestimate would approximately compensate for the statistical errors discussed above, and no corrections are necessary.

For energies greater than 800 GeV, the spectrum is averaged over all sizes and is approximately given by

$$N_n(>E) \sim E^{-1{\cdot}2}.$$

On integrating the energy spectrum of hadrons in an approximate manner, the percentage of the primary energy available in the hadronic component at 800 g cm^{-2} is found to be about 1·5% to 2·0% for $N_e < 3\times10^5$ and about 1·0% to 1·5% for $N_e > 3\times10^5$, the uncertainties arising from the shape of the spectrum at lower energies.

2.6. Fractional hadron energy spectrum

In figure 8 the integral energy spectra of hadrons of energy greater than 200 GeV are plotted for the same two size groups in a different way. The energy of the hadron is expressed as a fraction 'K' of the primary energy E_0 of the associated EAS. E_0 is calculated using the relation

$$E_0\,(\text{GeV}) = 2{\cdot}9\times10^6\left(\frac{N_e}{10^6}\right)^{0{\cdot}9}$$

where N_e is the number of electrons in the shower.

The number of hadrons per shower is obtained from the equation

$$N_n(>K) = F\sum_r \frac{T(r,>K)}{f(r)}$$

where F is the geometric factor of the cloud chamber, $f(r)$ is the observed flux per square metre of the showers at distance r and $T(r, >K)$ is the observed number of hadrons in the chamber of fractional energy greater than K at distance r from the core.

The experimental curves are compared with those expected for survivors of primaries calculated assuming different values of inelasticity and interaction mean free paths and different primary mass numbers. The detailed implications of such a comparison are discussed in paper II. The important point that we would like to stress at this juncture is that all sources of errors and biases tend to lower the experimental points or shift them towards lower K values. Thus any discrepancy between observation and calculation cannot be accounted for by such errors.

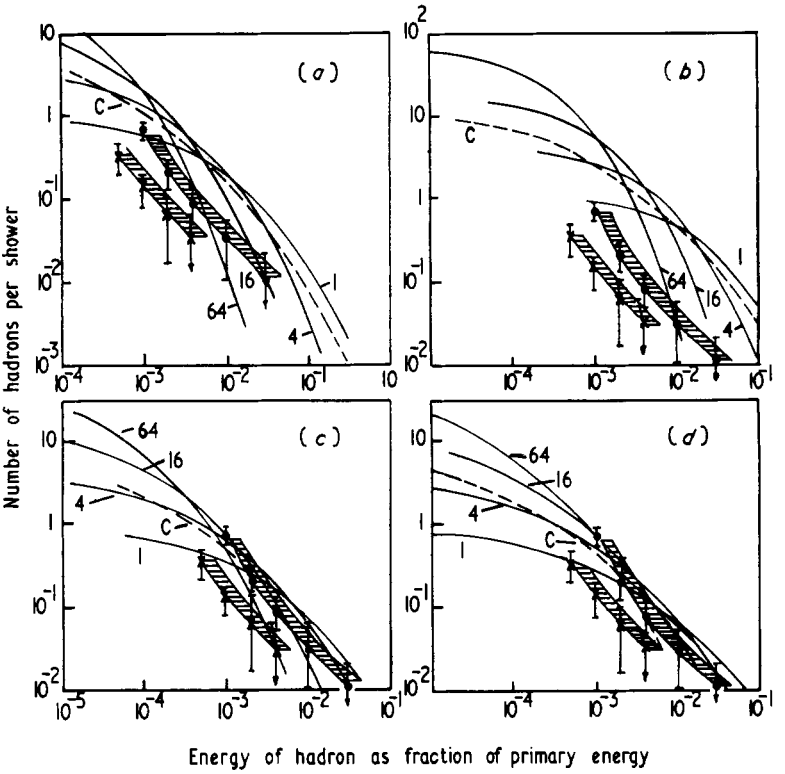

Figure 8. The fractional integral energy spectrum of high energy hadrons in EAS for the size groups less than $3{\cdot}2 \times 10^5$ (●) and greater than $3{\cdot}2 \times 10^5$ (×). The hadron energy is estimated as a fraction of the primary energy of the associated EAS. The experimental points are compared with the calculated integral energy spectra which are obtained for different values of elasticity (ϵ), interaction mean free path (λ) and atomic mass of primaries. Curves C represent a mixed composition approximating the one known at lower energies. The implications of such a comparison are discussed in a forthcoming paper. (*a*) $\lambda = 80\ \mathrm{g\,cm^{-2}}, \epsilon = 0{\cdot}5$; (*b*) $\lambda = 80\ \mathrm{g\,cm^{-2}}, \epsilon = 0{\cdot}6$; (*c*) $\lambda = 67\ \mathrm{g\,cm^{-2}}, \epsilon = 0{\cdot}5$; (*d*) $\lambda = 80\ \mathrm{g\,cm^{-2}}$. $\epsilon = 0{\cdot}4$.

2.7. The charge to neutral ratio of hadrons in EAS

The charge to neutral ratio (C/N) has been determined for different energies of hadrons at various distances from the core and for showers of different sizes. The procedure of acceptance of a hadron cascade for analysis is such that it is insensitive over a wide range to the actual value of the interaction mean free path of the hadron so that the detection efficiencies of charged and neutral events are nearly equal even if they have different interaction cross sections. The acceptance criteria for events to be identified as due to charged hadrons are: (i) the primary track must be identifiable as a single track in at least two compartments above the point of interaction; (ii) it must be uniquely identified from the detailed structure of the track in at least two views; (iii) the primary track direction must conform to the direction of the cascade axis within reasonable limits. To be identified as a neutral hadron the criteria adopted are: (i) the region above the point of interaction must be well within the illuminated and photographable region of the chamber; (ii) any track which could be mistaken as a likely charged primary in

one view, must be clearly eliminated as a stray track by reference to the other views. A final test before acceptance depends upon the answer to the following crucial question: 'Under exactly identical conditions, would the nature of the hadron be identified unambiguously if the primary was of the opposite type?' Many events which failed this test were rejected although they satisfied the other criteria. All the events were analysed twice. Twelve out of 874 events were found to be misidentified on re-analysis.

In table 3, the C/N ratios are given for three size and five energy groups. The figures in brackets correspond to weighted averages of the ratios in individual groups taking into account size variation and energy spectrum of hadrons. The unbracketed value is the ratio $\Sigma C/\Sigma N$. When hadrons of all energies greater than 25 GeV are combined, the ratio decreases from $6{\cdot}2 \pm 1{\cdot}3$ for sizes less than 3×10^5 to $3{\cdot}2 \pm 0{\cdot}5$ for sizes greater than 3×10^5 and then remains constant with increasing size. When combined for all sizes the ratio decreases with energy becoming $1{\cdot}1 \pm 0{\cdot}5$, for energies greater than 200 GeV where the geometric mean energy is about 300 GeV. In table 4, the ratios are given as a function of distance from the core for different energies but combined for all sizes. The energy estimate for the lowest energy group (10–25) GeV is inaccurate, and also possibly this energy group may be contaminated by recoil nucleons of energies less than 10 GeV, the extent of contamination depending upon distance from core and

Table 3. Charge to neutral ratio of hadrons in EAS—variation with shower size and hadron energy

Energy / Size	10–25 GeV	25–50 GeV	50–100 GeV	100–200 GeV	> 200 GeV	For all energies > 25 GeV
$< 3{\cdot}2 \times 10^5$	18/7 $2{\cdot}6 \pm 1{\cdot}2$	52/3 17 ± 10	70/12 $5{\cdot}8 \pm 1{\cdot}8$	21/9 $2{\cdot}3 \pm 0{\cdot}9$	5/4 $1{\cdot}2 \pm 0{\cdot}8$	148/28 $5{\cdot}3 \pm 1{\cdot}1$ $(6{\cdot}2 \pm 1{\cdot}3)$
$3{\cdot}2 \times 10^5$ to $1{\cdot}8 \times 10^6$	77/8 $9{\cdot}6 \pm 3{\cdot}6$	138/44 $3{\cdot}1 \pm 0{\cdot}5$	146/46 $3{\cdot}2 \pm 0{\cdot}5$	39/24 $1{\cdot}6 \pm 0{\cdot}4$	5/4 $1{\cdot}2 \pm 0{\cdot}8$	328/118 $2{\cdot}8 \pm 0{\cdot}3$ $(3{\cdot}1 \pm 0{\cdot}5)$
$> 1{\cdot}8 \times 10^6$	55/13 $4{\cdot}2 \pm 1{\cdot}3$	112/29 $3{\cdot}9 \pm 0{\cdot}8$	66/25 $2{\cdot}6 \pm 0{\cdot}6$	16/6 $2{\cdot}7 \pm 1{\cdot}3$	0/1	194/61 $3{\cdot}2 \pm 0{\cdot}5$ $(3{\cdot}3 \pm 0{\cdot}5)$
For all sizes	150/28 $5{\cdot}4 \pm 1{\cdot}1$ $(5{\cdot}2 \pm 1{\cdot}7)$	302/76 $4{\cdot}0 \pm 0{\cdot}5$ $(3{\cdot}7 \pm 0{\cdot}7)$	282/83 $3{\cdot}4 \pm 0{\cdot}4$ $(2{\cdot}9 \pm 0{\cdot}4)$	76/39 $2{\cdot}0 \pm 0{\cdot}4$ $(2{\cdot}1 \pm 0{\cdot}4)$	10/9 $1{\cdot}1 \pm 0{\cdot}5$	670/207 $3{\cdot}2 \pm 0{\cdot}3$

Table 4. Charge to neutral ratio of hadrons in EAS—variation with distance from core

Distance \ Energy	10–25 GeV	25–50 GeV	50–100 GeV	100–200 GeV	10–200 GeV
< 8 m	72/8 $9{\cdot}0 \pm 3{\cdot}4$	169/42 $4{\cdot}0 \pm 0{\cdot}7$	194/58 $3{\cdot}4 \pm 0{\cdot}5$	61/27 $2{\cdot}3 \pm 0{\cdot}5$	496/135 $3{\cdot}7 \pm 0{\cdot}4$
> 8 m	78/20 $3{\cdot}9 \pm 1{\cdot}0$	133/34 $3{\cdot}9 \pm 0{\cdot}8$	88/25 $3{\cdot}5 \pm 0{\cdot}8$	15/12 $1{\cdot}3 \pm 0{\cdot}5$	314/91 $3{\cdot}5 \pm 0{\cdot}4$

shower size. For the energy group 100–200 GeV, the small decrease seen in the ratio at large distances could be a consequence of the difference in $\langle p_T \rangle$ or difference in the height of production of pions and nucleons. Due to the flatter lateral distribution of hadrons at lower energies the arbitrary value of 8 m used may not be large enough to separate pions and nucleons in the energy interval (25–100) GeV.

3. Comparison of results

The results reported in this paper on high energy hadrons may be summarized as follows:

(i) There is a tendency for the lateral distribution of high energy hadrons to flatten with increasing size.

(ii) The energy spectrum of hadrons in the energy range 50–800 GeV may be expressed by a power law of the form

$$N_n(>E) = BE^{-\gamma(N_e)}$$

where γ increases with N_e from a value of 1·4 at 5×10^4 to 2·2 at 4×10^5 or more, and remains at this high value up to 3×10^6 particles at 800 g cm^{-2}. The corresponding values of γ, if the maximum probable systematic errors are considered, are 1·2 and 1·9 respectively.

(iii) The variation of the number of hadrons $N_n(>E)$ as a function of shower size N_e may be expressed as

$$N_n(>E) = AN_e^{\alpha(E)}.$$

It is found that $\alpha(E)$ decreases with increasing E from a value of about 0·8 at $E > 50$ GeV to about 0·4 at $E > 400$ GeV.

(iv) The fractional hadron energy spectrum for hadrons of energy greater than 200 GeV is different for showers of size less than 3×10^5 and greater than 3×10^5 particles.

(v) There are cases of hadrons of energy greater than a few TeV appearing at distances up to 5·6 m from the core of showers.

(vi) The charge to neutral ratio of hadrons decreases with increasing energy of hadrons. In showers of size less than 3×10^5 the ratio has a value $6{\cdot}2 \pm 1{\cdot}3$ for hadrons of energy greater than 25 GeV and the value is $1{\cdot}2 \pm 0{\cdot}8$ for hadrons of energy greater than 200 GeV. For showers of size greater than 3×10^5 the corresponding values are $3{\cdot}2 \pm 0{\cdot}5$ and $1{\cdot}2 \pm 0{\cdot}8$.

We shall now examine to what extent some of these results are supported by observations of others.

The flattening of the lateral distribution of hadrons with increasing size of the shower has been reported in a number of earlier experiments (Chatterjee *et al* 1968a, Hasegawa *et al* 1965, Miyake *et al* 1969). It has also been observed by us in the data from the TAS which was operated as a second hadron detector in the present experiment. In fact the tendency for flattening is much more pronounced in the TAS results. However, as discussed earlier, for a variety of reasons the multiplate cloud chamber results are more reliable. The tendency for flattening is also seen in the cloud chamber experiment of Kameda *et al* (1965) at sea level.

In figure 9, we have compared the results on the variation of the number of hadrons of different energy as a function of size reported in the different experiments. It is seen that the results from the TAS in the present experiment, which are in essential agreement with the TAS results of Chatterjee *et al* (1968a), show that the absolute number of hadrons

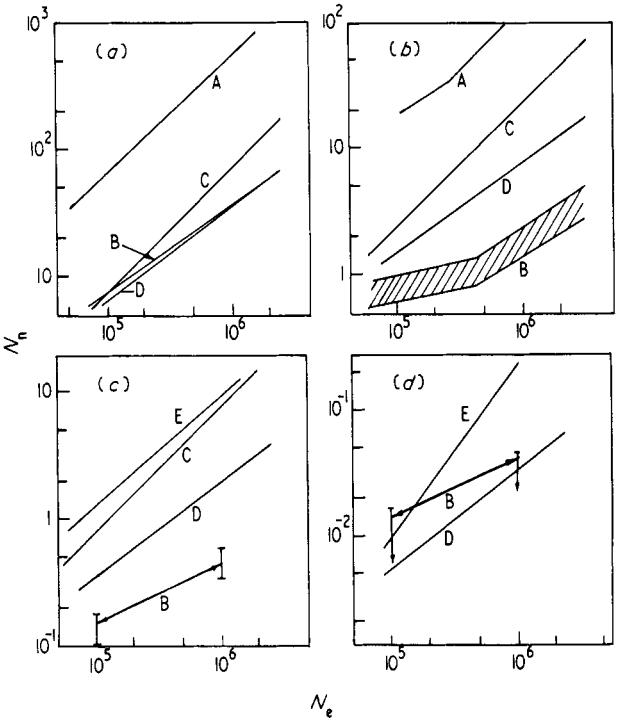

Figure 9. A comparison of the size variation of the number of hadrons with different energy thresholds obtained by various experimental groups using different hadron detectors. For clarity, statistical errors are not indicated in most of the results. (*a*) $E > 100$ GeV; (*b*) $E > 400$ GeV; (*c*) $E > 1$ TeV; (*d*) $E > 10$ TeV. In all four parts of the figure: curves A, present experiment (TAS); curves B, present experiment (Cl Ch); curves C, Kameda *et al* (1965); curves D, Miyake *et al* (1969); curves E, Matano *et al* (1969).

at energies greater than 100 and greater than 400 GeV are high compared to the cloud chamber results by more than an order of magnitude. We feel that the cloud chamber results on the flux and the spectrum of hadrons are more reliable than the TAS results for the following reasons. The cloud chamber has a much better spatial resolution and the energy of individual hadrons can be unambiguously determined by the method described by Vatcha *et al* (1972), even when multiple hadrons are incident which is generally the case with high energy hadrons close to the axis of shower. Also, the geometry in the cloud chamber experiment is well defined and only hadron interactions which occur well within the illumination region are considered for analysis. Since no visual detectors were used in conjunction with the TAS it was not possible to distinguish between the incidence of single high energy hadrons and multiple low energy hadrons and γ rays which can deposit an equal amount of energy. The abundance of such events is clearly revealed by the analysis of cloud chamber photographs obtained in the present experiment. The TAS, which is a more reliable instrument for measurement of energy when a single hadron is incident, thus reduces to an instrument for measuring the energy flow in hadrons and γ rays at short distances from the core. Also, because of leakage from the sides it becomes difficult to define precisely the aperture of the instrument. It may be pointed out that the results presented earlier on the time structure of hadrons using the TAS (Tonwar *et al* 1971) are not affected by these considerations, since in the

timing experiment mostly isolated events of energy about a few tens of GeV arriving up to distances of 20 m from the core were considered and the selection system was such that if the hadrons were associated even with a few prompt particles on the TAS, the events were rejected.

At a shower size of 10^5 particles, in the present experiment, in that of Miyake *et al* (1969) at Mt Norikura (2·8 km) and of Kameda *et al* (1965) at sea level, the number of hadrons of energy greater than 100 GeV is about 7. While there is agreement between the results of the present experiment and of Miyake *et al* regarding the size variation of the number of hadrons of energy greater than 100 GeV, the experiments of Kameda *et al* give a much faster rise. For hadrons of higher energy our results with the cloud chamber give a much lower value than those of Kameda *et al* and Miyake *et al*. In our experiment, as already stated, the energies of individual hadrons even at the highest energies are determined by the integral track length method using Monte Carlo simulations for calibration (Vatcha *et al* 1972). From the published papers the precise method adopted by others for the determination of energy of hadrons in the cloud chamber is not clear.

Our results on the variation of the number of hadrons with associated size N_e and energy of hadron E may be parametrized as follows:

$$N_n(>E, N_e) = 7{\cdot}3\left(\frac{N_e}{10^5}\right)^{0{\cdot}71}\left(\frac{E}{100}\right)^{\gamma} \qquad \text{for } (50 < E < 800)\,\text{GeV}$$

where

$$\gamma = \ln\left(\frac{N_e}{N_0}\right)^{-\alpha} \qquad \text{for } 5\times 10^4 < N_e < 4\times 10^5$$

and

$$\gamma = -\beta \qquad \text{for } 4\times 10^5 < N_e < 3\times 10^6$$

where

$$N_0 = 1{\cdot}4\times 10^3; \qquad \alpha = 0{\cdot}41, \qquad \beta = 2{\cdot}32.$$

For a maximum systematic underestimate of hadron energies by about 50 %, N_0, α, β may be altered to

$$N_0 = 1{\cdot}35\times 10^3; \qquad \alpha = 0{\cdot}33, \qquad \beta = 1{\cdot}88.$$

The break in the N_n against N_e curve at $N_e = (3\text{–}4)\times 10^5$ for high energy hadrons is not very significant statistically in our experiment; however, similar effects have been observed for low energy hadrons (few GeV) by Chatterjee (1964) and Danilova *et al* (1964) and also for low energy muons ($\sim$ 1 GeV) by Chatterjee *et al* (1968b). The results of Kameda *et al* on high energy hadrons do not show a break in the N_n against N_e curve. Their observations are at sea level and for showers of size greater than 10^5 particles. In our experiment the indication of a break is at about 3×10^5 particles at 800 g cm^{-2}. Since the break should ultimately be connected with the energy per nucleon of the primary particle, the break at 3×10^5 at 800 g cm^{-2} could occur at say about 10^5 at sea level. Since the observations of Kameda *et al* do not extend below 10^5, they cannot confirm or negate the evidence for a break. In most of the earlier experiments with non-visual detectors the slope of the integral hadron energy spectrum over a wide band of energies was found to be about 1·0 independent of shower size. The experiments of Miyake *et al* at 2·8 km showed a steepening of the spectrum, the slope changing to

about 1·8, beyond 500 GeV. The results of Matano *et al* (1969) at sea level have shown that at energies greater than 1·7 TeV, the slope changes to about 2·1. In our results the steepening is apparent even at lower energies.

The tendency for the charge to neutral ratio for hadrons to decrease with increasing energy is seen in the results of Kameda *et al* also. However, the results differ in absolute values. The ratios given by Kameda *et al* for all sizes are

$6{\cdot}0 \pm 1{\cdot}0$ for $E < 500$ GeV;

$2{\cdot}5^{+1{\cdot}5}_{-0{\cdot}5}$ for $E > 500$ GeV;

and

$1{\cdot}5 \pm 0{\cdot}5$ for $E > 1000$ GeV.

In our experiment, the ratio decreases to $1{\cdot}1 \pm 0{\cdot}5$ at $E > 200$ GeV. As already pointed out in connection with the discrepancy in the absolute number of hadrons, differences in the estimation of energy of hadrons in the two experiments may explain to some extent the discrepancies in the absolute values of C/N ratios also.

The evidence for a change in the value of C/N ratio for high energy hadrons as a function of shower size and distance from core and a distinct difference in the fractional hadron energy spectra for showers of size less than and greater than 3×10^5 particles and the steepening of the hadron spectra with size are important features that have been revealed by the present experiment which have not been reported by other investigators.

The implications of these various results on high energy hadrons in air showers from the point of view of the primary composition and strong interaction characteristics at ultra-high energies are discussed in the following papers.

Acknowledgments

We wish to thank Dr B K Chatterjee for collaboration in the early stages of the experiment. It is a pleasure to acknowledge the profitable discussions with Professor S Naranan, Drs G T Murthy, M V Srinivasa Rao, K Sivaprasad and S C Tonwar at various stages. Sri N V Gopalakrishnan carried out the tedious job of analysing several thousands of cloud chamber photographs. Technical services were provided by Sri A R Apte and Sri S G Khairatkar.

References

Chatterjee B K 1964 *PhD Thesis* University of Bombay

Chatterjee B K *et al* 1968a *Can. J. Phys.* **46** S136–41

—— 1968b *Can. J. Phys.* **46** S131–5

Danilova T V, Denisov E V and Nikolsky S I 1964 *Sov. Phys.–JETP* **19** 1056–66

Feynman R P 1969 *Phys. Rev. Lett.* **23** 1415–7

Hasegawa H, Noma M, Suga K and Toyoda Y 1965 *Proc. 9th Int. Conf. on Cosmic Rays, London* vol 2 (London: The Institute of Physics and The Physical Society) pp 642–5

Kameda T, Maeda T, Oda H and Sugihara T 1965 *Proc. 9th Int. Conf. on Cosmic Rays, London* vol 2 (London: The Institute of Physics and The Physical Society) pp 681–4

Matano T, Machida M and Ohta K 1969 *Proc. 11th Int. Conf. on Cosmic Rays, Budapest* vol 3 (Budapest: Central Research Institute for Physics) pp 451–62
Miyake S *et al* 1969 *Proc. 11th Int. Conf. on Cosmic Rays, Budapest* vol 3 (Budapest: Central Research Institute for Physics) pp 463–9
Murthy G T 1967 *PhD Thesis* University of Bombay
Ramana Murthy P V, Sreekantan B V, Subramanian A and Verma S D 1963 *Nucl. Instrum. Meth.* **23** 245–54
Tonwar S C and Sreekantan B V 1971 *J. Phys.* A: *Gen. Phys.* **4** 868–82
Vatcha R H 1972 *PhD Thesis* University of Bombay
Vatcha R H, Sreekantan B V and Tonwar S C 1972 *J. Phys.* A: *Gen. Phys.* **5** 859–76